RIP2 enhances cell survival by activation of NF-κB in triple negative breast cancer cells.

Rola Jaafar[a,1], Katarzyna Mnich[a], Sarah Dolan[a], Jennifer Hillis[a], Aitor Almanza[a], Susan E. Logue[a], Afshin Samali[a], Adrienne M. Gorman[a]*

Affiliation:

[a]Apoptosis Research Centre, National University of Ireland Galway, Ireland;

Corresponding author: Adrienne Gorman, Apoptosis Research Centre, School of Natural Sciences, National University of Ireland Galway, Ireland; Adrienne.gorman@nuigalway.ie

[1] Department of Surgery, American University of Beirut Medical Center, Beirut, Liban

Abstract

Receptor-interacting protein 2 (RIP2) is an essential mediator of inflammation and innate immunity, but little is known about its role outside the immune system. Recently, RIP2 has been linked to chemoresistance of triple negative breast cancer (TNBC), the most aggressive breast cancer subtype for which there is an urgent need for targeted therapies. In this study we show that high expression of RIP2 in breast tumors correlates with a worse prognosis and a higher risk of recurrence. We also demonstrate that RIP2 confers TNBC cell resistance against paclitaxel and ceramide-induced apoptosis. Overexpression of RIP2 lead to NF-κB activation, which contributed to higher expression of pro-survival proteins and cell survival. Conversely, RIP2 knockdown inhibited NF-κB signaling, reduced levels of anti-apoptotic proteins and sensitized cells to drug treatment. Together, these data show that RIP2 promotes survival of breast cancer cells through NF-κB activation and that targeting RIP2 may be therapeutically beneficial for treatment of TNBC.

Introduction

Receptor-interacting protein kinase 2 (RIP2/RICK/CARDIAK) is an important mediator of innate and adaptive immunity [1]. Structurally, RIP2 is composed of a N-terminal kinase domain, linked via an intermediate domain to a C-terminal caspase activation and recruitment domain (CARD). RIP2 signaling is most associated with the NOD-like receptor protein family where it is a core component of the NOD1 and NOD2 signaling pathways [2]. Following activation by specific bacterial peptides, NOD1 and NOD2 receptors recruit RIP2 via homotypic CARD-CARD interactions, leading to RIP2 autophosphorylation and K63-linked polyubiquitination at K209 within its kinase domain [3–5]. Once polyubiquitinated, RIP2 recruits TAK1 and IKK complexes leading to phosphorylation of IκB kinases and subsequent activation of NF-κB [4].

Our current knowledge of RIP2 signaling is primarily within the context of its role in innate and adaptive immunity. Recently, Singel and colleagues reported a role for RIP2 in breast cancer, particularly in triple negative breast cancer (TBNC), where it was linked to cell metastasis, migration and resistance to the chemotherapeutic docetaxel [6]. TNBC comprises ~15% of all breast cancers but is the most clinically challenging with a poor prognosis [7]. Since TNBC lacks targeted therapies and often becomes resistant to chemotherapies, new treatment approaches are urgently needed. In this study, we report elevated RIP2 expression in TNBC cell lines and in basal-like primary breast cancer samples. High expression of RIP2 correlated with a worse prognosis and a higher incidence of tumor recurrence. We link elevated RIP2 expression to increased cell death resistance and long-term survival post-treatment of TNBC cells with ceramide or paclitaxel. Our results indicate the protective influence of RIP2 is a consequence of NF-κB activation as repression of NF-κB signaling blocked RIP2-dependent induction of anti-apoptotic proteins and sensitized cells to cytotoxic treatment. Our

findings underscore the potential importance of RIP2 signaling in TNBC and highlight the need for further studies to understand the therapeutic potential of targeting RIP2 in TNBC.

Experimental Procedures:

Materials

All chemicals were from Sigma-Aldrich unless otherwise indicated.

Cell culture

MCF7 (ECACC), MDA-MB-231 (ATCC) and HEK293T (ATCC) cells were maintained in high glucose DMEM. T47D (ECACC), SKBR3 (ECACC), MDA-MB-453 (ATCC), MDA-MB-468 (ATCC) and BT-549 (ATCC) were maintained in RPMI. All media was supplemented with 10% FBS, 1% L-glutamine and 50 units/mL penicillin and 50 ug/mL streptomycin. MCF-10A (ATCC) were maintained in DMEM/F-12 supplemented with 5% horse serum, 20 ng/ml epidermal growth factor, 100 ng/ml cholera toxin, 0.01 mg/ml insulin and 500 ng/ml hydrocortisone. Cells were maintained at 37 °C, 5% CO_2 in a humidified atmosphere. For experiments, MDA-MB-231 cells were seeded at 30,000 cells/cm^2 24 h prior transfection and treatment with 30 µM ceramide or 1 µM paclitaxel.

Patient sample RIP2 qPCR

Primary breast cancer tissue samples luminal A (Lum A) (n=5), luminal B (Lum B) (n=4), HER2 (n=2), basal (n=5) were obtained from Dr. Róisín Dwyer, Department of Surgery, University College Hospital Galway, Ireland. RNA extraction was performed total mammalian RNA extraction kit (Qiagen) according to the manufacturer's protocol, 2 µg total RNA was reverse transcribed using 20 U Superscript II Reverse Transcriptase (Invitrogen). qPCR reactions were performed using SYBR-green Master Mix and the StepOne Plus platform (Applied Biosystems). RIP2 transcript levels were normalized to the average Ct of control

genes, PPIA and MRPL19, using the ΔΔCt method. Results are displayed as RIP2 abundance relative to tumor associated non-tumoral tissue.

Primer sequences for qPCR

RIP2	Forward	GATATCGAAATGAACCGCCT
	Reverse	CATGCTTTTATTTTGAAGTAA
PPIA	Forward	CATCCTAAAGCATACGGGTCC
	Reverse	TCTTTCACTTTGCCAAACACC
MRPL19	Forward	CTTAGGAATGTTATCGAAGGACAAG
	Reverse	GCTATATTCAGGAAGGGCATCT

Patient sample cohort *RIP2* expression analysis

Datasets were obtained from a cohort of 295 breast cancer patients of the Netherlands Cancer Institute (NKI-295) for which clinical data were available [8]. Gene expression data were statistically analyzed using R programming and GraphPad Prism. For survival analysis *RIP2* mean expression was used to divide patients into high and low *RIP2* groups and Kaplan-Meier curves were compared using a log-rank test (Mantel-Haenszel test). To compare *RIP2* levels across multiple breast cancer subtype groups, Analysis of Variance (ANOVA) test followed by Tukey's multiple comparisons test was utilized.

Generation of plasmid constructs

The N-terminal VSV-tagged RIP2 and CARD only RIP2 (DN RIP2) constructs were generated by PCR. K209R RIP2 mutant was generated by PCR-based site-directed mutagenesis. RIP2 constructs were cloned into pcDNA3.1+ (Invitrogen) using the EcoRI and XhoI sites. The NF-κB-GFP reporter pGreenFire1-P (System Biosciences) was cloned into the lentiviral vector

pWPT (Addgene). The fidelity of all constructs was confirmed by sequencing (LGC Genomics). Scrambled and RIP2 shRNA were purchased from GeneCopoeia. pRC-β-actin and the IκBα S32/36A-pRC-β-actin (NF-κB super-repressor) plasmids were a kind gift from Dr. Aideen Ryan, REMEDI, NUI Galway, Ireland.

Transient transfection of cells

Constructs were transfected into MDA-MB-231 cells using Turbofect transfection reagent (Fisher Scientific) according to the manufacturer's instructions. The culture medium was replaced at 4 h post-transfection and 20 h later cells were treated as indicated.

Immunoblotting

Cells were lysed in 20 mM HEPES pH=7.5, 350 mM NaCl, 1 mM MgCl$_2$, 0.5 mM EDTA, 0.1 mM EGTA, 0.1% Nonidet P-40) supplemented with protease and phosphatase inhibitors (PMSF, Aprotinin, NaF and Na$_3$VO$_4$). Protein concentration was measured using Bradford reagent with bovine serum albumin as a standard. Proteins were separated by SDS-PAGE and transferred onto nitrocellulose membranes. For immunoblotting membranes were blocked for 1 h in PBS containing 0.05% Tween 20 and 5% (w/v) non-fat dried milk and probed with antibodies against RIP2, XIAP, BCL-2, BCL-XL, cIAP1/2 (Santa Cruz), phospho-IκB and BAX (Cell Signalling Technologies), ACTIN (Sigma), followed by incubation with horseradish peroxidase (HRP)-conjugated secondary antibody (Jackson ImmunoResearch Laboratories) (1:10,000). Protein bands were visualized using chemiluminescent reagent (Pierce). Quantitative densitometric analysis of immunoblotting results was performed using ImageJ software.

Cell viability assay

MDA-MB-231 cells were incubated with 0.5 mg/ml of 3-(4,5-dimethythiazol2-yl)-2,5-diphenyl tetrazolium bromide (MTT) for 3 h at 37 °C. To stop the reaction and solubilize the

formazan crystals 20% (w/v) SDS in 50% (v/v) dimethyl formamide was added and the absorbance measured at 550 nm by a Victor3 microplate reader (Perkin Elmer Life Sciences). Cell viability was expressed as percent of viable cells relative to the control.

Clonogenic survival

Cells were seeded at a density of 1,000 cells per well in a 6-well plate a day before transfection. Transfected cells were treated with drug and 24 h later the media was changed. Cells were grown for 15 days with a change of medium every 3 days. Colonies were fixed, stained with 0.2% crystal violet in 20% methanol, rinsed with PBS and dried. Colonies containing >50 cells were counted.

Changes in mitochondrial transmembrane potential (ΔΨm)

Following treatment cells were harvested, incubated with 100 nM tetramethylrhodamine ethyl ester (Molecular Probes) for 30 min at room temperature and analyzed at 582 nm using FACSCanto flow cytometer (Becton Dickinson).

DEVDase activity

Caspase-3-like (DEVDase) activity was determined fluorometrically as reported previously [9].

Generation of a NF-κB-GFP reporter MDA-M-231 cell line

Lentivirus packaging plasmids psPAX2.2, pMD2.G and pRSV-rev (Addgene) along with a construct containing NF-κB-responsive transcriptional elements upstream of the *Firefly* luciferase gene were transfected into HEK293T cells using JetPEI transfection reagent (Polyplus) according to the manufacturer's instructions. Viral infection was carried out by spinoculation followed by incubation of MDA-MB-231 cells with virus-containing media for 18 h. NF-κB reporter MDA-MB-231 cells were selected using 4 μg/ml puromycin for 1 week.

Measurement of NF-κB activity

Luciferase activity was measured using One-Glo™ Luciferase assay (Promega) according to the manufacturer's instructions. Luminescence was measured at 560 nm on Victor3 microplate reader (Perkin Elmer) and normalized to control.

Statistical analysis

Statistical analysis was carried out using SPSS software. Data are represented as the mean ± SEM from individual experiments carried out at least in triplicate. Data were analyzed using repeated-measures ANOVA followed by multiple comparisons *post hoc* test. Differences were considered statistically significant at *$p < 0.05$; **$p < 0.01$; ***$p < 0.001$; ****$p < 0.0001$.

Results and discussion

High expression of RIP2 associates with basal-like breast cancers and with a worse overall patient survival.

To assess RIP2 expression in breast cancer cells we examined RIP2 protein levels in a panel of breast cancer cell lines, encompassing the main subtypes, and the non-tumorigenic breast epithelial cell line MCF-10a. We found expression of RIP2 protein to be elevated in those cell lines representative of TNBC namely MDA-MB-231, MDA-MB-453, MDA-MB-468 and BT549 cells (Figure 1A).

Examination of *RIP2* transcript levels in RNA derived from primary patient tissue samples (classified using molecular subtypes) determined the highest levels to be present in the basal subtype compared to luminal (Lum A and B), HER2 positive and tumor associated non-tumoral tissue (Figure 1B). Analysis of *RIP2* status in breast cancer subtypes using publicly available online data sets from a cohort of 295 patients of the Netherlands Cancer Institute (NKI-295)

[8] showed a similar trend with the highest *RIP2* expression present in basal-like breast cancers (Figure 1C). High *RIP2* expression status in breast tumors associated with significantly worse patient overall survival (p<0.001) (Figure 1D) and recurrence (p<0.01) (Figure 1E).

RIP2 protects MDA-MB-231 cells from ceramide and paclitaxel induced apoptosis

To understand the significance of RIP2 expression in TNBC we overexpressed wild-type RIP2 (WT RIP2), a ubiquitin conjugation-defective mutant of RIP2 (K209R) incapable of activating NF-κB, and a dominant negative form of RIP2 containing only the CARD domain (DN RIP2) in MDA-MB-231 cells (Figure 2A). Overexpression of WT RIP2 increased the viability of MDA-MB-231 cells compared to empty vector (EV) controls following treatment with either ceramide or paclitaxel (Figure 2B). In contrast, expression of the K209R mutant, while increasing RIP2 protein expression to a level similar to that observed with WT RIP2, failed to increase cell viability post-ceramide or paclitaxel treatment (Figure 2A-B), suggesting a requirement for NF-κB signaling in RIP2-mediated protection. Similarly, reduction of RIP2 signaling, via expression of DN RIP2, further decreased cell viability in ceramide and paclitaxel treated cells when compared to EV controls (Figure 2B). Additionally, we also reduced RIP2 levels in MDA-MB-231 cells by transfecting *RIP2* targeting shRNA (Figure 2A). Knockdown of *RIP2* significantly decreased cell viability in response to paclitaxel or ceramide treatment compared to scrambled control-transfected cells (Figure 2B).

To test if elevated RIP2 expression conferred long-term protection we carried out clonogenic assays. MDA-MB-231 cells transfected with EV or WT RIP2 were treated with ceramide or paclitaxel for 24 h after which the drug was removed, the cells washed and cultured for a further 15 days. Overexpression of RIP2 significantly increased colony number compared to EV controls demonstrating RIP2 overexpression confers long-term protection following ceramide or paclitaxel treatment (Figure 2C). Collectively, these results underscore the contribution of

RIP2 signaling to the viability of MDA-MB-231 cells following treatment either with ceramide or paclitaxel.

To understand how RIP2 regulates cell viability we examined apoptosis signaling by assessing loss of mitochondrial membrane potential (ψ_m) and effector caspase activation (DEVDase activity). Overexpression of WT RIP2 significantly suppressed apoptosis signaling as illustrated by maintenance of ψ_m and suppression of effector caspase activation upon paclitaxel or ceramide treatment (Figure 2D-E). In agreement with this, reducing RIP2 expression, via transfection with *RIP2* shRNA, amplified apoptosis signaling post-ceramide or paclitaxel treatment compared to scrambled controls (Figure 2D-E). These results indicate that elevated RIP2 expression may contribute to the suppression of cell death triggered by paclitaxel or ceramide in MDA-MB-231 cells.

RIP2 increases expression of anti-apoptotic proteins and confers cell protection via NF-κB signaling

Regulation of BCL-2 protein family members and inhibitors of apoptosis proteins (IAPs) controls the onset of apoptosis signaling [10]. Given the suppression of mitochondrial-mediated death and effector caspase activity observed upon RIP2 overexpression we next examined whether RIP2 increased levels of pro-survival proteins. Overexpression of RIP2 increased XIAP, BCL-2 and BCL-XL levels, and decreased levels of the pro-apoptotic protein BAX, in MDA-MB-231 cells (Figure 3A-B). Conversely, *RIP2* knockdown decreased XIAP, cIAP1/2, BCL-2 and BCL-XL expression and increased levels of BAX (Figure 3A-B). This indicates that high RIP2 expression increases levels of anti-apoptotic proteins and that lowering RIP2 expression may help prime MDA-MB-231 cells for death induced by chemotherapeutics such as paclitaxel.

Given the link between RIP2 and NF-κB activation [4] and that elevated NF-κB activity has previously been described in TNBC cells and linked to their chemo-resistance [11] we asked if the observed alterations in protein expression were a consequence of NF-κB signaling. To this end, we generated MDA-MB-231 cells stably expressing a luciferase reporter construct with a NF-κB responsive element. Overexpression of WT RIP2 in reporter cells increased NF-κB promoter activity, in contrast to K209R or DN RIP2 whose overexpression did not increase promoter activity, but tended to reduce it (Figure 4A). Knockdown of RIP2 reduced NF-κB reporter activity compared to scrambled controls (Figure 4A). To underscore the relationship between RIP2 and NF-κB we transfected the MDA-MB-231 N-FκB reporter cells with RIP2 and non-degradable IκBα S32/36A mutant (NF-κB SR). Overexpression of NF-κB SR inhibited luciferase reporter activity (Figure 4B). This was accompanied by reduced phosphorylation of IκB and a concomitant reduction in RIP2-dependent increase in expression of XIAP, BCL-2 and BCL-XL (Figure 4C). Suppression of RIP2-mediated NF-κB activation also reduced the ability of RIP2 overexpression to rescue MDA-MB-231 cell viability following ceramide treatment (Figure 4D). These data suggest that increased expression of RIP2 in MDA-MB-231 cells contributes to constitutive NF-κB activation leading to elevated levels of anti-apoptotic proteins and conferring cell death resistance.

Further studies are required to define the mechanisms facilitating activation of RIP2 signaling in breast cancer cells. In addition to NODs, RIP2 activation has also been reported to occur through interactions with the p75 neurotrophin receptor (p75^{NTR}), components of the TNFR1 and the CD40 receptor complexes [1,12,13]. Nerve growth factor (NGF)-dependent p75^{NTR} signaling has already been linked to the suppression of ceramide-induced MDA-MB-231 cell death [14]. Given that MDA-MB-231 cells secrete basal levels of NGF and that NGF has been demonstrated to enhance RIP2 interaction with p75^{NTR} in HEK293 cells [14] it is tempting to consider a potential contribution of NGF and p75^{NTR} in RIP2 activation in breast cancer cells.

Whether these interactions contribute to RIP2-mediated resistance of MDA-MB-231 cells to cytotoxic drugs remains to be determined.

Aside from delineating the biology of RIP2 in breast cancer, there is an importance for assessing the therapeutic potential of targeting RIP2 in TNBC. It is tempting to speculate that either targeting RIP2 expression or interfering with RIP2 polyubiquitination at K209 could be viable therapeutic strategies to reduce pro-survival NF-κB signaling and therefore increase the susceptibility of TNBC breast cancer cells to cytotoxic agents. Given that RIP2 kinase activity is important for maintenance of RIP2 stability [15], targeting RIP2 for degradation using RIP2 kinase inhibitors may also be a potential therapeutic approach.

In summary, our findings, in combination with the previous work by Singel and colleagues [6], suggest a strong rationale for further investigating the impact of RIP2 signaling in breast cancer and in particular TNBC.

References

[1]   A.I. Chin, P.W. Dempsey, K. Bruhn, J.F. Miller, Y. Xu, G. Cheng, Involvement of receptor-interacting protein 2 in innate and adaptive immune responses, Nature. 416 (2002) 190–194. doi:10.1038/416190a.

[2]   K. Kobayashi, N. Inohara, L.D. Hernandez, J.E. Galán, G. Núñez, C.A. Janeway, R. Medzhitov, R.A. Flavell, RICK/Rip2/CARDIAK mediates signalling for receptors of the innate and adaptive immune systems., Nature. 416 (2002) 194–9. doi:10.1038/416194a.

[3]   M. Dorsch, A. Wang, H. Cheng, C. Lu, A. Bielecki, K. Charron, K. Clauser, H. Ren, R.D. Polakiewicz, T. Parsons, P. Li, T. Ocain, Y. Xu, Identification of a regulatory autophosphorylation site in the serine–threonine kinase RIP2, Cell. Signal. 18 (2006) 2223–2229. doi:10.1016/J.CELLSIG.2006.05.005.

[4]   M. Hasegawa, Y. Fujimoto, P.C. Lucas, H. Nakano, K. Fukase, G. Núñez, N. Inohara, A critical role of RICK/RIP2 polyubiquitination in Nod-induced NF-κB activation, EMBO J. 27 (2008) 373–383. doi:10.1038/sj.emboj.7601962.

[5]   J.T. Tigno-Aranjuez, J.M. Asara, D.W. Abbott, Inhibition of RIP2's tyrosine kinase activity limits NOD2-driven cytokine responses., Genes Dev. 24 (2010) 2666–77. doi:10.1101/gad.1964410.

[6]   S.M. Singel, K. Batten, C. Cornelius, G. Jia, G. Fasciani, S.L. Barron, W.E. Wright, J.W. Shay, Receptor-interacting protein kinase 2 promotes triple-negative breast cancer cell migration and invasion via activation of nuclear factor-kappaB and c-Jun N-terminal kinase pathways., Breast Cancer Res. 16 (2014) R28. doi:10.1186/bcr3629.

[7]   S. Badve, D.J. Dabbs, S.J. Schnitt, F.L. Baehner, T. Decker, V. Eusebi, S.B. Fox, S. Ichihara, J. Jacquemier, S.R. Lakhani, J. Palacios, E.A. Rakha, A.L. Richardson, F.C.

Schmitt, P.-H. Tan, G.M. Tse, B. Weigelt, I.O. Ellis, J.S. Reis-Filho, Basal-like and triple-negative breast cancers: a critical review with an emphasis on the implications for pathologists and oncologists, Mod. Pathol. 24 (2011) 157–167. doi:10.1038/modpathol.2010.200.

[8]   M. Arc, J. Van De, V. Ijver, Y. Udong, A.J. Van 't, V. Eer, H. Ongyue, D. Ai, A. Ugustinus, A.M.H. Art, D. Orien, W. V Oskuil, G. Eorge, J.S. Chreiber, J. Ohannes, L.P. Eterse, C. Hris, R. Oberts, M. Atthew, J.M. Arton, M. Ark, P. Arrish, D. Ouwe, A. Tsma, A. Nke, W. Itteveen, A. Nnuska, G. Las, L. Eonie, D. Elahaye, T. Ony, V. Der, V. Elde, H. Arry, B. Artelink, S. Joerd, R. Odenhuis, E. Miel, T.R. Utgers, S. Tephen, H.F. Riend, R. Ené, B. Ernards, A GENE-EXPRESSION SIGNATURE AS A PREDICTOR OF SURVIVAL IN BREAST CANCER, N Engl J Med. 347 (2002). http://www.nejm.org/doi/pdf/10.1056/NEJMoa021967 (accessed December 21, 2017).

[9]   K. Mnich, L.A. Carleton, E.T. Kavanagh, K.M. Doyle, A. Samali, A.M. Gorman, Nerve growth factor-mediated inhibition of apoptosis post-caspase activation is due to removal of active caspase-3 in a lysosome-dependent manner., Cell Death Dis. 5 (2014) e1202. doi:10.1038/cddis.2014.173.

[10]   R. Rathore, J.E. McCallum, E. Varghese, A.-M. Florea, D. Büsselberg, Overcoming chemotherapy drug resistance by targeting inhibitors of apoptosis proteins (IAPs), Apoptosis. 22 (2017) 898–919. doi:10.1007/s10495-017-1375-1.

[11]   N.M. Patel, S. Nozaki, N.H. Shortle, P. Bhat-Nakshatri, T.R. Newton, S. Rice, V. Gelfanov, S.H. Boswell, R.J. Goulet, G.W. Sledge, H. Nakshatri, Paclitaxel sensitivity of breast cancer cells with constitutively active NF-κB is enhanced by IκBα super-repressor and parthenolide, Oncogene. 19 (2000) 4159–4169. doi:10.1038/sj.onc.1203768.

[12]   I. Charalampopoulos, A. Vicario, I. Pediaditakis, A. Gravanis, A. Simi, C.F. Ibáñez, Genetic Dissection of Neurotrophin Signaling through the p75 Neurotrophin Receptor, Cell Rep. 2 (2012) 1563–1570. doi:10.1016/J.CELREP.2012.11.009.

[13]   J. V McCarthy, J. Ni, V.M. Dixit, RIP2 is a novel NF-kappaB-activating and cell death-inducing kinase., J. Biol. Chem. 273 (1998) 16968–75. doi:10.1074/JBC.273.27.16968.

[14]   A. Witt, D. Vucic, Diverse ubiquitin linkages regulate RIP kinases-mediated inflammatory and cell death signaling, Cell Death Differ. 24 (2017) 1160–1171. doi:10.1038/cdd.2017.33.

[15]   C. Nembrini, J. Kisielow, A.T. Shamshiev, L. Tortola, A.J. Coyle, M. Kopf, B.J. Marsland, The kinase activity of Rip2 determines its stability and consequently Nod1- and Nod2-mediated immune responses., J. Biol. Chem. 284 (2009) 19183–8. doi:10.1074/jbc.M109.006353.

Figure legends:

FIGURE 1. High expression of RIP2 in Triple Negative Breast Cancer associates with a poor prognosis and survival. (A) Protein lysates from a panel of breast cancer cell lines and the non-tumorigenic breast epithelial MCF10A cells were immunoblotted for RIP2 and ACTIN. **(B)** qPCR quantification of the *RIP2* mRNA levels in BC patient samples obtained from luminal subtype A and B tumor tissues (Lum A and B), HER2 (human epidermal growth factor receptor 2), basal-like tumor (basal) and relative to tumor associated non-tumoral tissue (TA). **(C)** Distribution of high and low *RIP2* mean expression of public BC expression array datasets within the indicated BC subtypes. **(D)** Kaplan-Meier overall survival curve and **(E)**

relapse-free survival based on *RIP2* mean expression in breast tumors. Relapse-free survival is defined as being local recurrence, regional recurrence, second primary tumor or distant metastasis.

FIGURE 2. RIP2 reduces sensitivity of MDA-MB-231 cells to ceramide and paclitaxel. **(A)** Protein lysates from cells expressing empty vector (EV), wild-type RIP2, K209R RIP2 mutant (K209R), CARD-only RIP2 (dnRIP2), scrambled shRNA (sc) and RIP2 shRNA (shRIP2) were immunoblotted for RIP2 and ACTIN. *non-specific band. **(B-D)** Cells expressing RIP2 constructs were treated with 30 µM ceramide or 1 µM paclitaxel. **(B)** The effect on cell viability was assessed 24 h later. **(C)** Clonogenic survival was examined 15 days after treatment. The effect on **(D)** ψ_m and **(E)** DEVDase activity was assessed 24 h later.

FIGURE 3. RIP2 regulates expression of pro-survival and pro-apoptotic proteins. (A-B) MDA-MB-231 cells were transfected with EV, RIP2, scrambled control and RIP2 shRNA (shRIP2). **(A)** Protein extracts were immunoblotted for RIP2, XIAP, cIAP1/2, BCL-XL, BCL-2, BAX, ACTIN. **(B)** Densitometric and statistical analysis of the indicated protein expression was carried out. Data shown are normalized to ACTIN and relative to control.

FIGURE 4. RIP2 enhances cell survival by increasing NF-κB activity. (A,B) MDA-MB-231 NF-κB luciferase reporter cells were transfected either with **(A)** EV, RIP2, scrambled shRNA and RIP2 shRNA constructs or **(B)** with EV and RIP2 in the presence or absence of NF-κB SR. The effect on NF-κB activity was assessed 24 h post-transfection. **(C)** Protein extracts from MDA-MB-231 cells co-transfected with RIP2 and NF-κB SR were immunoblotted for RIP2, p-IκB, XIAP, BCL-2, BCL-XL and ACTIN. **(D)** Cells expressing EV or RIP2 were treated with 30 µM ceramide and cell viability was determined 24 h later. Values shown are relative to EV control.
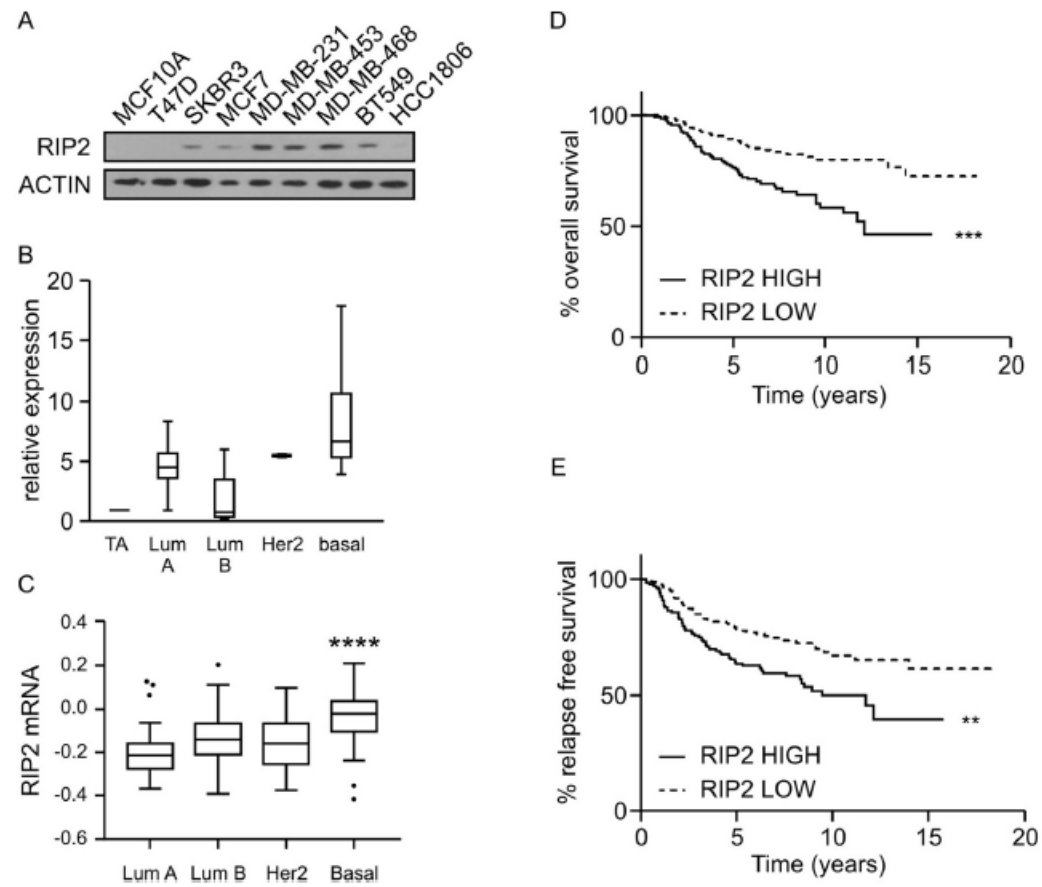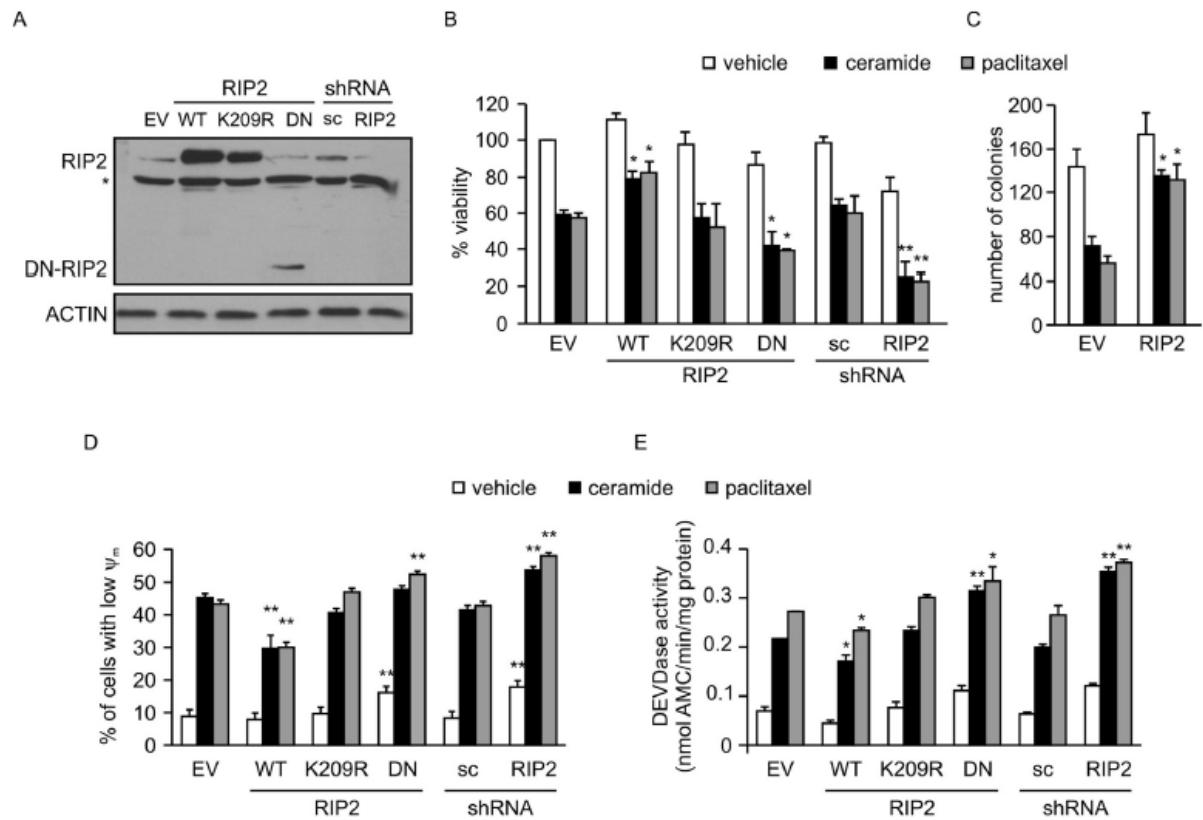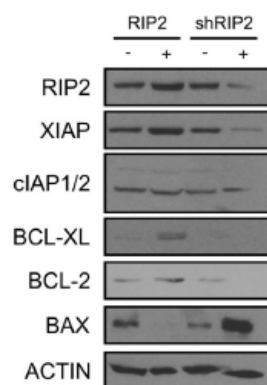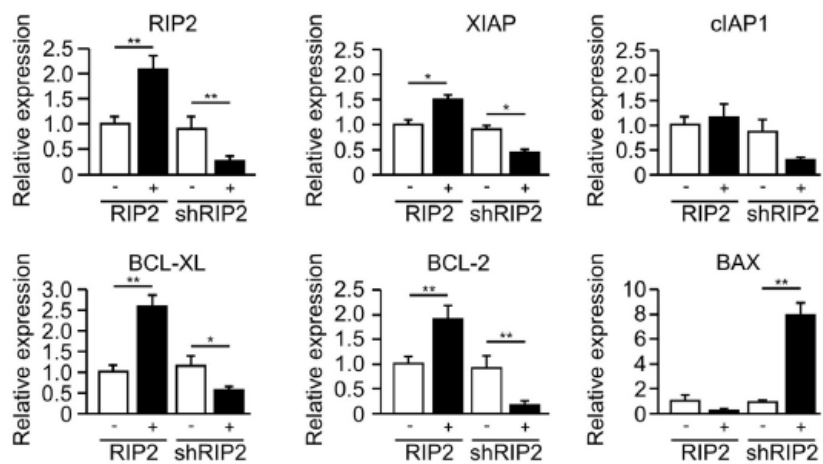
Figure 1

Figure 2

Figure 3

Figure 4